Vaporizing gravity currents in a superheated porous medium

By ANDREW W. WOODS

School of Mathematics, University of Bristol, Bristol, BS8 1TW, UK

We analyse the motion of a current of water migrating under gravity into a hot vapour-saturated porous rock accounting for the vaporization which occurs as the water invades the hot rock. We present a series of similarity solutions to describe the rate of advance of both planar and axisymmetric currents when the total mass of water injected after time t is proportional to t^γ. Three distinct cases arise. When $\gamma > 1/2$ (planar) or $\gamma > 1$ (axisymmetric), the depth of the current increases at all points from the source, and therefore vaporization occurs at all points on its surface. This case is described by a simple extension of the well-known similarity solutions for non-vaporizing currents. When $0 < \gamma < 1/2$ (planar) or $0 < \gamma < 1$ (axisymmetric), there is a region near the source where the depth of the current decreases. The depth only increases at the more distant points. Vaporization therefore only occurs in the leading part of the current where it is advancing into the superheated rock. In this case, we develop modified similarity solutions which account for the vaporization in the distal part of the current. The third case involves the finite release of fluid. Owing to the vaporization, the mass of the current decreases with time. Since there is no injection, the rate of advance of the current can no longer be found by comparing the exponents of time in the local and global equations for mass conservation. Instead, the motion is described by a class of similarity solutions of the second kind, analogous to those described by Barenblatt (1997), in which the total mass of the current is proportional t^γ, where γ is a function of the mass fraction which vaporizes, $\mathscr{F}$, such that $\gamma \to 0$ as $\mathscr{F} \to 0$ and $\gamma \to -1$ as $\mathscr{F} \to 1$. The model is extended to include the effects of capillary retention of fluid in the pore spaces and we discuss the relevance of our results to the process of liquid reinjection in the geothermal power industry.

1. Introduction

Power is generated from vapour-saturated geothermal reservoirs by drawing vapour from the reservoir and passing it through turbines and heat exchangers. Important commercial reservoirs include the Geysers reservoir in California, the Wairaki reservoir in New Zealand and the Lardarello field in Italy. In order to maintain the useful operating life of such reservoirs, vapour must be continually regenerated in the reservoir and to this end water is often injected into the reservoir. To improve understanding of this reinjection process, a number of theoretical and experimental studies have analysed vapour production as water invades the hot permeable reservoir rock (Fitzgerald & Woods 1994, 1995; Pruess *et al.* 1987; Woods & Fitzgerald 1993, 1997). The relevance of such porous flow models for geothermal systems has been described in more detail by Fitzgerald & Woods (1995), who argue that it provides

a useful simplification for modelling flow through a multiply fractured rock, and we adopt this model herein.

The studies have shown that as liquid invades a superheated porous layer, the heat transfer from the hot matrix to the liquid may cause some vaporization. The mass fraction which vaporizes depends upon the superheat of the reservoir and the rate of advance of the liquid front in comparison with the speed of both (i) the isotherms in the liquid and (ii) the isobars in the vapour (Woods & Fitzgerald 1993, 1997). In superheated permeable rocks, pressure anomalies migrate through the rock according to a nonlinear diffusion equation with effective diffusivity $D_P = KP_\infty/\phi\mu \sim 10^{-2}$ m^2 s^{-1} where $P_\infty \sim 10^6$ Pa is the far-field pressure and $\mu \sim 10^{-5}$ Pa s is the vapour viscosity (Fitzgerald & Woods, 1995) while heat is conducted through the system with diffusivity $\kappa \sim 10^{-6}$ m^2 s^{-1}. Since $D_P \sim 10^4\kappa$, it is possible for the liquid flow speed to be in excess of the thermal diffusion speed but to fall below the effective isobar diffusion speed. In this intermediate regime, there is a negligible amount of heat conduction from the far field and the interface pressure remains very close to that in the far field. The mass fraction of liquid which vaporizes is then determined by the superheat of the rock at the interface. The superheat is a function of the initial reservoir temperature and the interface temperature, which in this intermediate regime is approximately equal to the saturation temperature associated with the far-field pressure (Woods & Fitzgerald 1993). The mass fraction of liquid which vaporizes is therefore given by

$$\mathscr{F} = \frac{1}{1 + S\phi}, \tag{1.1}$$

where $S = L/C_p(T_s - T_b)$ is the ratio of the latent heat of vaporization L to the initial superheat of the rock, $C_p(T_s - T_b)$. In many geothermal systems, the rate of advance of the liquid–vapour interface has a value which lies in this intermediate regime. Therefore, in this paper, we restrict attention to situations in which condition (1.1) applies so that $\mathscr{F}$ may be assumed to be independent of time and position. In §7 we describe the range of liquid injection rates for which this approximation is valid, and show that these span most regimes of interest for geothermal systems.

Although the thermodynamics of the phase change and subsequent vapour motion have been studied in some detail, there has been little investigation of the dynamics of the liquid as it migrates through the porous layer and vaporizes. Instead, the liquid has been assumed to have a prescribed velocity field, corresponding to a planar, cylindrical or spherically spreading front. However, in many situations, gravity exerts a dominant control on the advance of the liquid region from the source. For example, in some preliminary numerical calculations of the motion of water leaving a source, Pruess *et al.* (1991) has shown that a downward sinking plume falls to the base of the reservoir where it spreads out under gravity. In the present work, we examine the dynamics of vaporizing liquid currents spreading under gravity, and we develop a series of similarity solutions to describe the motion.

We focus on the spreading of a source of water along the horizontal base of a reservoir and consider both planar and radially symmetric currents. These represent end-member models for a range of different reservoir geometries. The case of constant injection rate (§3) involves a simple re-interpretation of the solutions for non-vaporizing currents (Huppert & Woods 1995), and the present discussion extends the analysis of Woods & Fitzgerald (1995). The more complex case of a waning injection rate is described by a new class of similarity solutions in which only the leading part of the current vaporizes (§4). The case of a finite release with no injection is described

by similarity solutions of the second kind in which the decay rate depends on the mass fraction vaporizing (§5). The models have some connection with the classic model of liquid slumping in a porous layer with non-zero capillary forces (Barenblatt 1997). In §6, we extend the approach to include the effects of both capillarity and vaporization. Although the solutions are equivalent, our formulation of the problem differs from that of Barenblatt in that we use global mass conservation for the solutions of both the first and second kind; in contrast Barenblatt (1997) introduced an additional boundary condition when seeking similarity solutions of the second kind.

2. Non-vaporizing gravity currents

2.1. *Uni-directional currents*

The motion of non-vaporizing planar gravity currents in porous layers has been described by Barenblatt (1952), Bear (1971) and Huppert & Woods (1995). A planar gravity current, propagating in the x-direction, with depth $y = h(x, t)$, in a layer of uniform permeability K and porosity ϕ with fluid of viscosity μ may be described by the relations (figure 1)

$$\phi \frac{\partial h}{\partial t} + \frac{\partial}{\partial x}(uh) = 0 \tag{2.1}$$

and

$$u = -\frac{K\rho g}{\mu}\frac{\partial h}{\partial x}, \tag{2.2}$$

where g is the gravitational acceleration and ρ is the fluid density. If the total volume of fluid injected up to time t is $Q_o t^\gamma$ (per unit width of current), then global conservation of mass requires

$$\phi \int_0^{L(t)} h(x, t)\mathrm{d}x = Q_o t^\gamma, \tag{2.3}$$

where $L(t)$ is the current length and $h(L(t), t) = 0$. In addition, local conservation of mass at the source requires

$$\gamma Q_o t^{\gamma-1} = -\frac{K\rho g}{\mu}\left[h\frac{\partial h}{\partial x}\right] \quad \text{at} \quad \eta = 0. \tag{2.4}$$

Huppert & Woods (1995) have demonstrated that this system admits similarity solutions of the form

$$h = H(Dt)^\alpha f(\eta), \tag{2.5}$$

where $H = (Q_o/S^\gamma)^{1/(2-\gamma)}$, $D = (S^2/Q_o)^{1/(2-\gamma)}$, $S = K\rho g/\mu$ and $\eta = x/H(Dt)^\beta$. In these solutions, the shape factor $f(\eta)$ satisfies the equation

$$\phi\left(\alpha f - \eta\beta\frac{\mathrm{d}f}{\mathrm{d}\eta}\right) = \frac{\mathrm{d}}{\mathrm{d}\eta}\left(f\frac{\mathrm{d}f}{\mathrm{d}\eta}\right) \tag{2.6}$$

and the exponents α and β are related according to $\alpha = 2\beta - 1$. The global conservation of mass reduces to

$$\phi \int_0^\lambda f(\eta)\mathrm{d}\eta = 1 \tag{2.7}$$

and α and β are related to γ according to $\alpha + \beta = \gamma$. Note therefore that in the limit $\gamma = 2$, $HD = S$ and $h = Stf(\eta)$ (cf. (2.5)).
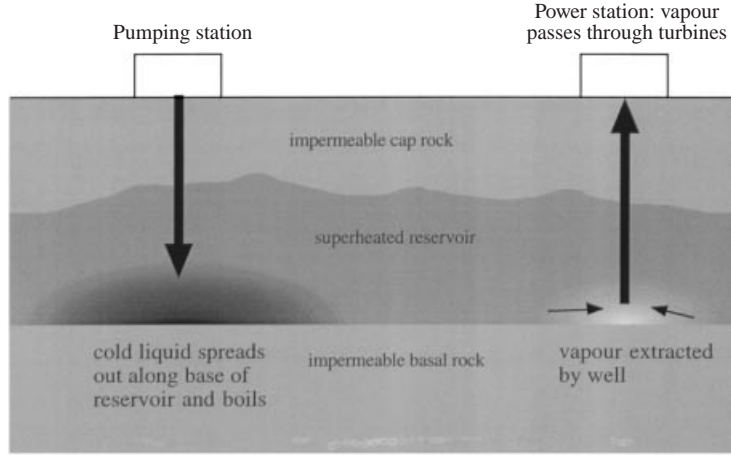
FIGURE 1. Schematic illustrating the evolution of a vaporizing gravity current in which the leading part of the current ascends and vaporizes while the trailing part of the current descends.

Conservation of mass at the source requires

$$f\frac{\mathrm{d}f}{\mathrm{d}\eta}\bigg|_0 = -\gamma \tag{2.8}$$

and the leading edge of the current is located at position $\eta = \lambda$ where $f(\lambda) = 0$. In these solutions, the current ascends throughout its length when $\partial h/\partial t > 0$ for $0 < \eta < \lambda$, and this requires $\gamma > 1/2$. If $\gamma < 1/2$, then the current descends near the source and only ascends near the leading edge.

Note that such solutions are only physically relevant once the current has spread sufficiently that $L(t) \gg H(Dt)^\alpha$ and the hydrostatic approximation (cf. (2.2)) applies. Indeed, laboratory experiments show that once $L(t) \geqslant H(Dt)^\alpha$, these similarity solutions provide a very accurate description of the flow (Huppert & Woods 1995).

A simple but instructive fundamental solution to this nonlinear problem arises in the case of a finite release of fluid. Now $\gamma = 0$, $\alpha = -\beta = -1/3$ and the shape of the current is (Pattle 1959)

$$f(\lambda) = (\lambda^2 - \eta^2)/6 \tag{2.9}$$

with $\lambda = (9/\phi)^{1/3}$. In this solution, $\partial h/\partial t = 0$ at $\eta = 3^{-1/2}\lambda$.

2.2. Radial currents

The motion of radial non-vaporizing gravity currents is described in a similar manner. If r is the radial coordinate, then the mass conservation equation (2.1) becomes

$$\phi r\frac{\partial h}{\partial t} + \frac{\partial hru}{\partial r} = 0 \tag{2.10}$$

while the velocity field is still given by equation (2.2). If the volume injected after time t is $Q_o t^\gamma$, then the current is described by similarity solutions of the form $h = H_a(D_a t)^\alpha f_a(\eta_a)$, $\eta_a = r/H_a(D_a t)^\beta$ where $H_a = (Q_o/S^\gamma)^{1/(3-\gamma)}$ and $D_a = (S^3/Q_o)^{1/(3-\gamma)}$. The shape factor f_a satisfies the modified similarity equation

$$\phi\left(\alpha\eta_a f_a - \beta\eta_a^2\frac{\mathrm{d}f_a}{\mathrm{d}\eta_a}\right) = \frac{\mathrm{d}}{\mathrm{d}\eta_a}\left(\eta_a f_a\frac{\mathrm{d}f_a}{\mathrm{d}\eta_a}\right) \tag{2.11}$$

with boundary conditions

$$-2\pi\eta_a f_a \frac{\mathrm{d}f_a}{\mathrm{d}\eta_a} = \gamma \quad \text{at} \quad \eta_a = 0, \tag{2.12}$$

and at the leading edge of the current, $\eta_a = \lambda_a$, the depth $f_a(\lambda_a) = 0$. The exponents α and β again satisfy the relation $\alpha = 2\beta - 1$.

The global conservation of mass has the form

$$2\pi\phi \int_0^{\lambda_a} \eta f_a(\eta)\mathrm{d}\eta = 1 \tag{2.13}$$

and the exponents α and β are related to γ according to $\alpha + 2\beta = \gamma$. It is readily seen that if $\gamma > 1$ then the current ascends throughout its length, $\partial h/\partial t > 0$ for $0 < \eta < \lambda_a$.

Again, there is an instructive analytical solution corresponding to the case of a finite release of fluid, $\gamma = 0$. In this case $\alpha = -2\beta = -1/2$ and f_a has the form (Barenblatt 1952)

$$f_a(\eta_a) = (\lambda_a^2 - \eta_a^2)/8, \tag{2.14}$$

where $\lambda_a = (6/\pi\phi)^{1/3}$.

We now build upon this model to describe the motion of such currents when they invade a superheated reservoir and partially vaporize.

3. Vaporizing gravity current

As a gravity current spreads through a superheated geothermal system, a fraction of the liquid may vaporize; in all solutions below we assume that the fraction which vaporizes is a constant $\mathscr{F}$ as explained in §1. The vaporization modifies the motion of the residual current. Two different regimes may occur depending on the rate of injection. If the liquid injection rate is sufficiently high then the interface ascends everywhere as the current spreads and a constant fraction $\mathscr{F}$ of the injected liquid vaporizes. However, if the liquid injection rate is slower, then the liquid near the source descends and vaporization only occurs near the leading edge of the current as it invades the hot rock. We first analyse the fast injection case for which the whole interface ascends and produces vapour. In §4, we consider the more complex slow-injection case in which only the leading part of the current vaporizes. In §6 we extend the analysis to include the possible effects of capillary retention of fluid in the pores as well as boiling at the front.

3.1. *One-dimensional currents*

If throughout the current, $\partial h/\partial t > 0$, then a fraction $\mathscr{F}$ of the current vaporizes at each position along its upper surface, and the rate of deepening of the current is given by

$$\phi\frac{\partial h}{\partial t} = (1 - \mathscr{F})\frac{K\rho g}{\mu}\frac{\partial}{\partial x}\left(h\frac{\partial h}{\partial x}\right). \tag{3.1}$$

Also, if the total volume injected after time t is $Q_o t^\gamma$ per unit width, then the global conservation of mass satisfies the equation

$$(1 - \mathscr{F})Q_o t^\gamma = \phi \int_0^{L(t)} h\mathrm{d}x, \tag{3.2}$$

where the leading edge of the current, $x = L(t)$, has zero depth, $h(L(t), t) = 0$. As in §2, such currents may be described by similarity solutions of the form $h(x, t) =$
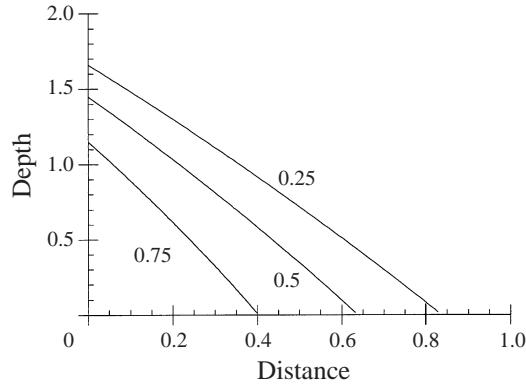
FIGURE 2. Shape of a self-similar uni-directional current, $f(\eta)$, propagating from a constant source of fluid in the cases $\mathscr{F} = 0.25, 0.5$ and 0.75. The current profiles are shown at that time at which the equivalent non-vaporizing current would extend unit distance from the source.

$H_v(D_v t)^\alpha f_v(\eta)$ (e.g. Huppert & Woods, 1995) but subject to the constraint

$$\partial h/\partial t > 0, \tag{3.3}$$

where $\eta = x/H_v(D_v t)^\beta$ with $\alpha = (2\gamma - 1)/3$ and $\beta = (\gamma + 1)/3$. The constraint (3.3) requires that throughout the current

$$H_v D_v^\alpha t^{\alpha-1} \left(\alpha f_v(\eta) - \beta\eta \frac{\mathrm{d}f_v}{\mathrm{d}\eta} \right) > 0. \tag{3.4}$$

Since the current becomes progressively shallower with distance from the source, $\partial h/\partial t > 0$ throughout the current if it is positive at the source, $\eta = 0$. Therefore this model applies when $\alpha > 0$ and hence $\gamma > 1/2$.

If H_v and D_v are defined as (cf. §2)

$$H_v = \left(Q_o(1 - \mathscr{F})^{(1-\gamma)}/S^\gamma \right)^{1/(2-\gamma)} = H(1 - \mathscr{F})^{(1-\gamma)/(2-\gamma)} \tag{3.5}$$

and

$$D_v = (S^2(1 - \mathscr{F})/Q_o)^{1/(2-\gamma)} = D(1 - \mathscr{F})^{1/(2-\gamma)} \tag{3.6}$$

then $f_v(\eta)$ is formally identical to the solution $f(\eta)$ presented in §2. The dependence of H_v and D_v on $\mathscr{F}$ identifies that the effect of the vaporization is identical to reducing both the effective supply rate, $Q_o t^\gamma$, and also the natural speed, $S = K\rho g/\mu$, of the current by the factor $1 - \mathscr{F}$. This fraction corresponds to that part of the injectate which remains as liquid. In figure 2, the profile of the spreading vaporizing current is shown for three values of $\mathscr{F}$ in the case $\gamma = 1$. As expected, for a given source flux, the depth and extent of the current increases as $\mathscr{F}$ decreases. Figure 3 illustrates the profile of the current for $\mathscr{F} = 0.25$ at three succesive times, showing how the interface ascends at all positions along the current as it advances forwards.

In the limiting case $\gamma = 1/2$ the interface has a fixed depth at the source, $x = 0$, but everywhere ahead of the source the interface ascends and therefore the above model may be used to describe the propagation. The case of slower injection rates, $\gamma < 1/2$, in which a part of the interface descends, is described in §5.

3.2. Radial currents

In the fast injection case, for which $\partial h/\partial t > 0$ throughout the current, the model of axisymmetric spreading currents (§2.2) may also be extended to account for vaporiza-
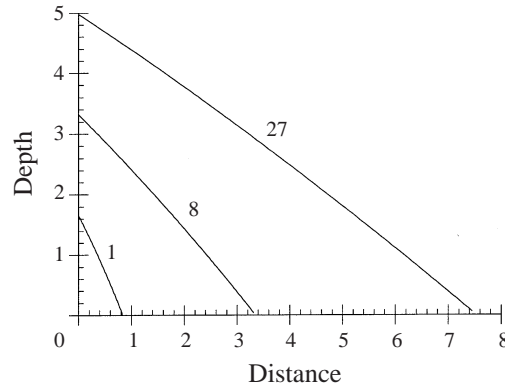
FIGURE 3. The evolution of the current profile at three dimensionless times 1, 8 and 27 showing how it becomes more elongate as it advances and deepens. This figure corresponds to injection at a constant rate with $\mathcal{F} = 0.25$. The injection rate is such that the equivalent non-vaporizing current would extend unit distance from the source at $t = 1$.

tion (cf. Woods & Fitzgerald, 1995). By analogy with uni-directional spreading and vaporizing currents (§3.1), the motion of an axisymmetrically spreading and vaporizing current is described by the similarity solutions of §2.2, $h = H_{av}(D_{av}t)^\alpha f_a(\eta)$, where H_{av} and D_{av} are now defined as (cf. (3.5), (3.6)) $H_{av} = \left(Q_o(1 - \mathcal{F})^{(1-\gamma)}/S^\gamma\right)^{1/(3-\gamma)}$ and $D_{av} = (S^3(1 - \mathcal{F})^2/Q_o)^{1/(3-\gamma)} = D(1 - \mathcal{F})^{2/(3-\gamma)}$. In the axisymmetric geometry, the condition $\partial h/\partial t > 0$ throughout the current requires $\gamma \geqslant 1$, and therefore includes the limiting case of a steady injection rate.

In figure 4, the profiles of three axisymmetric currents driven by a constant source of liquid, $\gamma = 1$, but corresponding to three values of $\mathcal{F}$, are shown. For such axisymmetric currents, the depth of the current increases as $f_a \sim (2|\ln\eta|)^{1/2}$ as $\eta \to 0$, in order to match the flux supplied from model source at $\eta = 0$. Although the similarity solution predicts that the current depth is singular at $r = 0$, the mass of fluid in the current near $r = 0$ is in fact negligible. Note that in a real system, the actual source would have finite size (e.g. a well-bore), $r = r_o$, so that current depth would be finite but time dependent at the source. The real current profile then asymptotes to the similarity solution ahead of the source.

As for the uni-directional currents, the size of the region filled with liquid increases for a given injection rate as $\mathcal{F}$ becomes smaller.

4. Slow injection – partially vaporizing currents

4.1. *Planar flow*

In §3, we identified that if the liquid supply rate is sufficiently slow, $0 < \gamma < 1/2$, then a region develops around the source where $\partial h/\partial t < 0$ so that the current descends and there is no vaporization. As the current descends, vapour flows into the pore spaces and cools. The temperature of this vapour may be inferred from that of the liquid. When the liquid is emplaced into the porous layer, it flows towards the boiling front and therefore, owing to the effects of thermal inertia, it rapidly attains the vaporization temperature (Pruess *et al.* 1987). The liquid remains close to the injection temperature only in a narrow boundary region near the source, of relative size ϕ (Woods & Fitzgerald 1996). Therefore, to good approximation, the vapour which replaces the descending liquid cools to the vaporization temperature and there
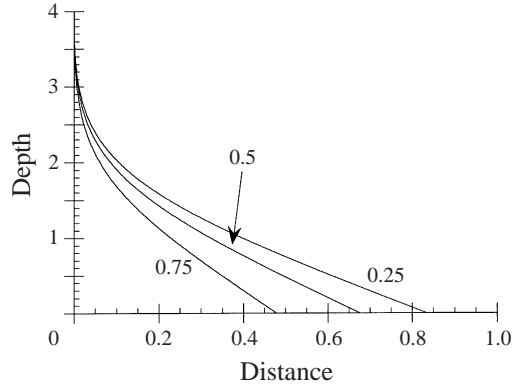
FIGURE 4. Profile of an axisymmetric current produced by a constant source of fluid for the values $\mathscr{F} = 0.25, 0.5$ and 0.75. In this axisymmetric geometry the current depth becomes singular at the origin corresponding to the source of fluid. The flow rate is chosen so that the equivalent non-vaporizing current would extend unit distance from the source.

is little condensation of the invading vapour. Note that some condensation may occur as liquid drains from the small region near the source which has been cooled to the liquid injection temperature; however, in a typical geothermal reservoir, this cold region represents a fraction $\sim \phi = 0.01$–0.1 of the region invaded by liquid and may therefore be neglected, to leading order.

In the region, $0 < x < L_1(t)$ say, in which the current is descending, h satisfies the equation

$$\phi \frac{\partial h}{\partial t} = \frac{K \rho g}{\mu} \frac{\partial}{\partial x} \left(h \frac{\partial h}{\partial x} \right) \tag{4.1}$$

while in the region $L_1(t) < x < L_2(t)$, in which the current is ascending, h satisfies the equation

$$\phi \frac{\partial h}{\partial t} = (1 - \mathscr{F}) \frac{K \rho g}{\mu} \frac{\partial}{\partial x} \left(h \frac{\partial h}{\partial x} \right). \tag{4.2}$$

The point $x = L_1(t)$ dividing the ascending and descending regions is defined by $\partial h / \partial t = 0$. At the leading edge of the current, $x = L_2(t)$, the current depth $h = 0$ while at the source, $x = 0$, the conservation of mass requires $(K \rho g / \mu) h (\partial h / \partial x) = -\gamma Q_o t^{\gamma - 1}$ (cf. equation (2.4)).

If liquid is continually injected into the system, $\gamma > 0$, then the global conservation of mass may be expressed as

$$\gamma Q_o t^{\gamma - 1} = \phi \frac{\mathrm{d}}{\mathrm{d}t} \int_0^{L_2(t)} h \mathrm{d}x + \phi \frac{\mathscr{F}}{1 - \mathscr{F}} \int_{L_1(t)}^{L_2(t)} \frac{\partial h}{\partial t} \mathrm{d}x. \tag{4.3}$$

The first term on the right-hand side accounts for the advance of the current and the second term for the production of vapour.

Such currents may be described by similarity solutions, $h = H(Dt)^\alpha f_p(\eta)$, where $\eta = x / H(Dt)^\beta$ and H and D are as in §2.1. If the points $x = L_1(t)$ and $L_2(t)$ are denoted by $\eta = \lambda_1$ and λ_2 then the boundary conditions on the current may be expressed as
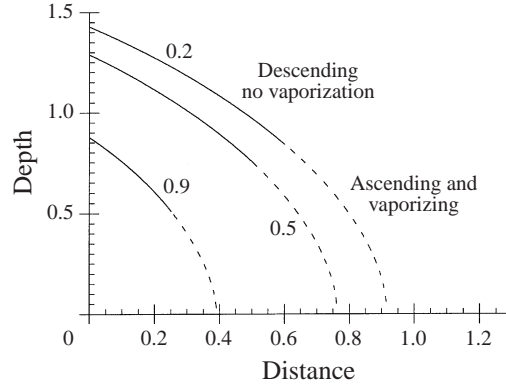
$$f_p(\lambda_2) = 0, \tag{4.4}$$

FIGURE 5. The profile of a planar current, $f_p(\eta)$, produced with an injection rate $1/t$ for $\mathscr{F} = 0.2, 0.5$ and 0.9. The region of the current which is descending is shown by the solid line, while the ascending leading edge of the current is shown by the dashed line.

$$f_p \mathrm{d}f_p/\mathrm{d}\eta \Big|_{\eta=0} = -\gamma. \tag{4.5}$$

At the point $\eta = \lambda_1$, f_p and $\mathrm{d}f_p/\mathrm{d}\eta$ are continuous and

$$\frac{\partial h}{\partial t}\Big|_{L_1(t)} = \alpha f_p(\lambda_1) - \beta\eta\frac{\mathrm{d}f_p}{\mathrm{d}\eta}\Big|_{\lambda_1} = 0. \tag{4.6}$$

The global conservation of mass (4.3) may be re-expressed as

$$\gamma = \phi \int_0^{\lambda_2} (\alpha f_p - \beta\eta f_p)\mathrm{d}\eta + \frac{\phi\mathscr{F}}{1-\mathscr{F}}\int_{\lambda_1}^{\lambda_2} (\alpha f_p - \beta\eta f_p)\mathrm{d}\eta. \tag{4.7}$$

When $\gamma > 0$, the area occupied by the current continually increases.

In the next section, §5, we describe the situation in which there is a finite release of fluid; in that case, owing to the vaporization, the volume of fluid continually decreases. However, the present model may in fact be extended for application to the intermediate case in which the area of the current remains constant (the first term on the right-hand side of (4.3) and (4.7) vanishes). For this to occur, we require $\mathrm{d}Q/\mathrm{d}t = Q_o/t$ so that the total volume injected from time t_o to t is $Q = Q_o \ln(t/t_o)$. This is of different functional form to the power law injection rates described above. Now, $\alpha = -1/3$, $\beta = 1/3$ and the left-hand side of (4.3) becomes Q_o/t, while the left-hand side of (4.7) becomes unity. Since the liquid saturated region is of fixed volume, the addition of new liquid at the source is exactly balanced by the vaporization at the leading edge of the current as it spreads along the base of the reservoir.

In figure 5, the current profile for three values of $\mathscr{F}$ is shown for the case $\mathrm{d}Q/\mathrm{d}t = Q_o/t$. The ascending part of the current, where vaporization occurs, is shown by the dashed lines, while the descending part of the current near the source is shown with solid lines. The current tends to steepen and occupies a smaller area as $\mathscr{F}$ increases. In §3 we showed that the effective speed of a vaporizing current is smaller than a non-vaporizing current by the factor $1 - \mathscr{F}$. This causes the leading part of the current, $\eta > \lambda_1$, to steepen as $\mathscr{F}$ increases and as a result of the greater vaporization the current fills a smaller volume.

Figure 6 illustrates the time evolution of the current for the case $\mathscr{F} = 0.5$. Again, the dashed part of the current surface denotes the region in which vaporization occurs.
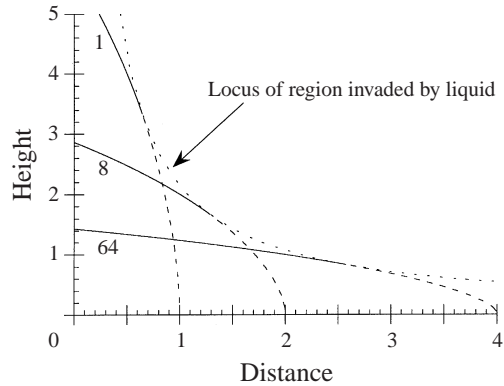
FIGURE 6. The shape of the current at the dimensionless times $t^* = 1, 8, 64$ for injection at a rate $1/t$ such that the current extends unit distance from the source at $t^* = 1$. For this injection rate, the area of the current remains constant, but the liquid-filled region continually migrates through the rock, with the leading edge invading new superheated rock (dashed lines), and the trailing part of the current descending (solid lines) to leave a region of rock which is just saturated. The locus of the region which is occupied with liquid at some point during the current evolution is shown by the dotted line.

As the rear of the current slumps, the point at which $\partial h/\partial t = 0$ and the current starts to vaporize, migrates forwards and downwards. As a result, a region of rock whose temperature is close to the saturation temperature develops above the current near the source. This is marked by the dotted line in figure 6. The thermal energy released from this region of rock when it was invaded by the current and cooled was used to vaporize the liquid injected at earlier times. Therefore, even though the region occupied by the current is of fixed area (in this two-dimensional current), the region of rock providing the heat for vaporization grows.

In the next section we consider the case in which there is no injection so that the area occupied by the current continually decreases.

4.2. *Radial flow*

The same approach may be used to describe the motion of partially vaporizing currents which are radially symmetric. For axisymmetric currents, whenever $0 < \gamma < 1$ a region near the source develops in which the current descends, $\partial h/\partial t < 0$. The shape function now satisfies the radially symmetric nonlinear diffusion equation (cf. §2), and as noted in §3.2, for finite injection rate the current depth becomes singular as $\eta \to 0$. Figure 7 illustrates the shape of such radially spreading currents for three values of $\mathscr{F}$ for the limiting injection rate $\mathrm{d}Q/\mathrm{d}t \sim Q_o/t$. Again, the leading part of the current, where vaporization occurs, is shown by the dashed line. As for the planar spreading current, the vaporization reduces the effective current propagation speed by the factor $1 - \mathscr{F}$ and so the leading edge of the flow steepens.

5. Vaporization of a current involving a finite release

5.1. *Planar currents*

When a finite release of fluid, injected at $t = 1$, spreads through a superheated domain, the mass of fluid in the current progressively decreases owing to the vaporization. As in the previous sections, to describe this motion, we seek similarity solutions of the form $h = H(Dt)^\alpha f_f(\eta)$ where $\eta = x/H(Dt)^\beta$ and $\alpha = 2\beta - 1$. However, since there is
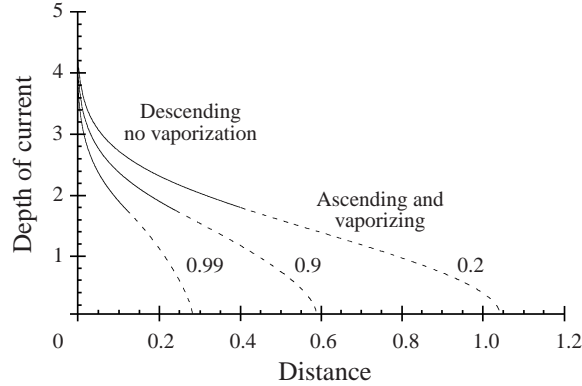
FIGURE 7. The profile of an axisymmetric spreading current supplied with fluid at a rate Q_o/t. Curves are shown for $\mathscr{F} = 0.2$, 0.9 and 0.99.

no further injection of liquid, the value of α does not simply emerge from comparison of the time exponents in the equation for the global conservation of mass (equation (4.3)). Instead, if the liquid region has volume $V_o t^\gamma$ per unit width, then the exponent γ now emerges as an eigenvalue for the problem and is therefore a function of the mass fraction which vaporizes, $\mathscr{F}$.

Before solving the problem, we first note from §2 that, with no vaporization, $\mathscr{F} = 0$, the solution (2.9) with $\alpha = -1/3$ describes the spreading of a current of finite mass and no injection, $\gamma = 0$. This suggests that if the current vaporizes as it spreads, then $\alpha < -1/3$ and $\gamma < 0$. Secondly, we note that in the limit $\mathscr{F} \to 1$, all the current vaporizes, $\beta \to 0$ and $\alpha, \gamma \to -1$. Therefore, we expect that for vaporizing currents produced from a finite release, γ lies in the range $-1 < \gamma < 0$ and α in the range $-1 \leqslant \alpha \leqslant 1/3$.

For each value of α, the shape factor $f_f(\eta; \mathscr{F})$ is the solution of the system

$$\phi\left(\alpha f_f - \beta\eta\frac{\mathrm{d}f_f}{\mathrm{d}\eta}\right) = \frac{\mathrm{d}}{\mathrm{d}\eta}\left(f_f\frac{\mathrm{d}f_f}{\mathrm{d}\eta}\right) \quad \text{for} \quad 0 < \eta < \lambda_1, \tag{5.1}$$

$$\phi\left(\alpha f_f - \beta\eta\frac{\mathrm{d}f_f}{\mathrm{d}\eta}\right) = (1 - \mathscr{F})\frac{\mathrm{d}}{\mathrm{d}\eta}\left(f_f\frac{\mathrm{d}f_f}{\mathrm{d}\eta}\right) \quad \text{for} \quad \lambda_2 > \eta > \lambda_1 \tag{5.2}$$

with boundary conditions

$$\frac{\mathrm{d}f_f}{\mathrm{d}\eta} = 0 \quad \text{at} \quad \eta = 0, \tag{5.3}$$

$$\alpha f_f - \beta\frac{\mathrm{d}f_f}{\mathrm{d}\eta}\eta = 0 \quad \text{and} \quad f_f(\eta-) = f_f(\eta+) \quad \text{at} \quad \eta = \lambda_1 \tag{5.4}$$

and

$$f_f = 0 \quad \text{at} \quad \eta = \lambda_2. \tag{5.5}$$

In order that the solution f_f is physically realisable, it should also satisfy the equation for global conservation of mass, (4.3), which for no injection may be expressed as

$$\int_0^{\lambda_2}\left(\alpha f_f - \beta\eta\frac{\mathrm{d}f_f}{\mathrm{d}\eta}\right)\mathrm{d}\eta + \frac{\mathscr{F}}{1 - \mathscr{F}}\int_{\lambda_1}^{\lambda_2}\left(\alpha f_f - \beta\eta\frac{\mathrm{d}f_f}{\mathrm{d}\eta}\right)\mathrm{d}\eta = 0. \tag{5.6}$$
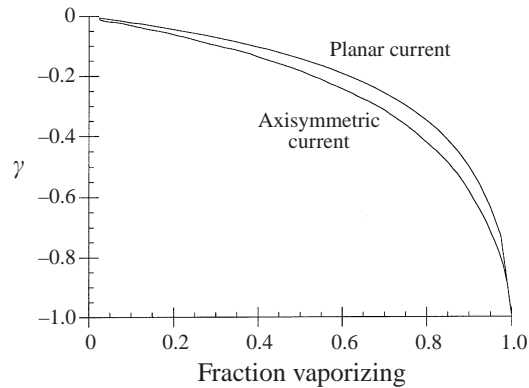
FIGURE 8. Variation of the exponent γ for a current of finite mass $Q_o t^\gamma$ released at $t = 1$, as a function of the mass fraction which vaporizes, $\mathscr{F}$. Results for both the planar and axisymmetric currents are shown.
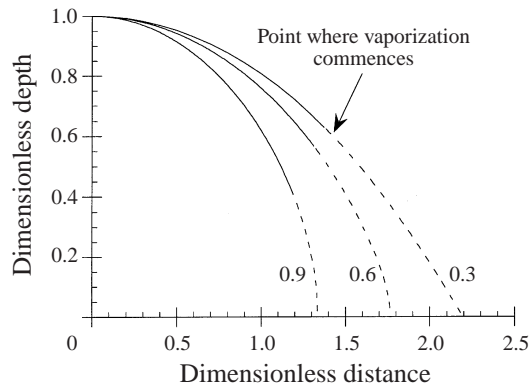

FIGURE 9. Profile of a planar current, released at $t = 1$, and spreading through a superheated porous layer in which the mass fraction which vaporizes is $\mathscr{F} = 0.3, 0.6$ and 0.9. Curves are shown for currents of depth $f = 1$ at $\eta = 0$.

For each value of $\mathscr{F}$, equation (5.6) follows directly from (5.1)–(5.5). Solution of (5.1)–(5.5) thus involves the selection of the value $\alpha(\mathscr{F})$ and hence $\gamma(\mathscr{F}) = (3\alpha + 1)/2$.

We have solved equations (5.1)–(5.6) numerically and in figure 8 we illustrate the variation of γ with $\mathscr{F}$. As expected, for small values of $\mathscr{F}$ the current decays slowly $|\gamma| \ll 1$ and therefore advances relatively rapidly along the ground. In contrast, in the limit $\mathscr{F} \to 1$, the current decays rapidly, $\gamma \to -1$, and hence advances very slowly, $\beta \ll 1$. Figure 9 illustrates the shape of the associated currents for several values of $\mathscr{F}$. As $\mathscr{F}$ increases, more of the current vaporizes as it invades the hot rock, and therefore the current becomes increasingly steep at the leading edge.

It is interesting to compare this solution method, based on the global equation for mass conservation, with that described by Barenblatt for the related problem of a finite volume of fluid spreading through a porous layer but with a fraction of the fluid remaining trapped in pore spaces by capillary action. Again the mass of the current gradually wanes with time, and the motion is described by similarity solutions of the second kind. Barenblatt (1997) derives these solutions by introducing a third boundary condition, rather than the equation for global conservation of mass; the third boundary condition, introduced at the leading edge of the current, follows from
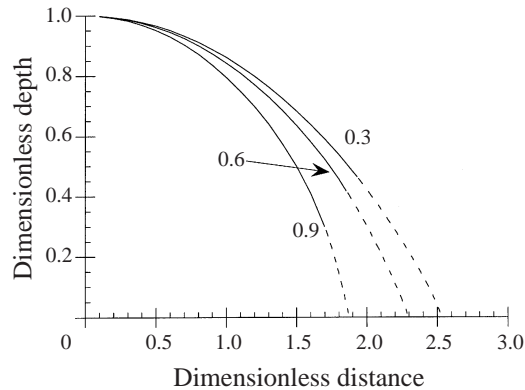
FIGURE 10. Profile of an axisymmetric current, released at $t = 1$, and spreading through a superheated porous layer in which the mass fraction which vaporizes is $\mathscr{F} = 0.3$, 0.6 and 0.9. Curves are shown for currents of depth $f = 1$ at $\eta = 0$.

(5.2) and has the form

$$\frac{\mathrm{d}f_f}{\mathrm{d}\eta} = -\frac{\phi\beta\lambda_2}{(1 - \mathscr{F})}.$$

This is directly analogous to our integral constraint, (5.6), which is readily derived by integrating (5.1) and (5.2) across the current. The advantage of the integral constraint is that the problem formulation is directly related to that described in §4 to find similarity solutions of the first kind in which the same equation for the global conservation of mass was adopted, but including a term for the source of fluid. Further details of the mathematical properties of these similarity solutions of the second kind may be found in the articles by Aronson & Vazquez (1994, 1995) and Hulshof & Vazquez (1994).

5.2. *Axisymmetric currents*

The axisymmetric motion of a finite release of fluid may also be described by a family of similarity solutions in which the total mass of the current has value $Q_o t^\gamma$ where $\gamma = \gamma(\mathscr{F})$ with $0 < \gamma < -1$. The shape function for the current, $f_a(\eta_a)$, is however described by the radially symmetric analogue of equations (5.1)–(5.6) (cf. §§2, 3). We now find that $\gamma \to 0$ and $\alpha \to 0$ as $\mathscr{F} \to 0$ while $\gamma \to -1$ and $\alpha \to -1/2$ as $\mathscr{F} \to 1$, and the curve $\gamma(\mathscr{F})$ is also shown in figure 8. For the axisymmetric current, $\gamma(\mathscr{F})$ is smaller than the equivalent value for the planar current as a result of the different geometry of the currents. It is worth noting that since there is no flux supplied to these axisymmetric currents, then in contrast to the solutions presented in §§3.2 and 4.2 (figures 4, 7), the depth of the current remains finite as $\eta_a \to 0$, as illustrated in figure 10.

6. Effects of capillarity

We have so far neglected the effects of capillarity, although some of the liquid may remain trapped in the pore spaces as the fluid sinks and spreads laterally. This trapped fraction, R, will depend on the interfacial tension and the pore size. In a uniform porous layer, after any transients associated with the descent of the liquid, the mass of trapped liquid is expected to be independent of position. Thus, although detailed discussion of this process is beyond the scope of the present analysis, it is interesting

to illustrate the possible effect of capillarity through a very simple model in which we assume the retained fraction of fluid takes a constant value R (cf. Barenblatt 1997). Now in any region in which $\partial h/\partial t < 0$, the equation governing the spreading of the current takes the modified form

$$(1 - R)\phi\frac{\partial h}{\partial t} = \frac{K\rho g}{\mu}\frac{\partial}{\partial x}\left(h\frac{\partial h}{\partial x}\right), \qquad (6.1)$$

while in the region in which the current ascends and boils, the motion is governed by equation (5.2). The boundary conditions at $\eta = 0, \lambda_1$ and λ_2 again depend on the flux condition at the source, but have the same form as described in §§4 and 5. As well as equation (6.1), the other main change to the model is the equation for the global conservation of mass (cf. (4.3)) which takes the modified form

$$\frac{dQ}{dt} = \phi\frac{d}{dt}\int_0^{L_2(t)} h\,dx - R\phi\int_0^{L_1(t)}\frac{\partial h}{\partial t}dx + \phi\frac{\mathscr{F}}{1-\mathscr{F}}\int_{L_2(t)}^{L_1(t)}\frac{\partial h}{\partial t}dx, \qquad (6.2)$$

where the new second term on the right-hand side accounts for the loss of fluid by capillary retention in the descending part of the flow.

The method of solution for this model is identical to that described in §§3–5, and depends on the injection rate. For fast injection (§3), the current ascends throughout its length, $L_1 = 0$ and no capillary retention occurs. For slower injection (§4), the effect of capillary retention is important near the source, where $\partial h/\partial t < 0$, and leads to a modification of the shape of the current, although the exponent of time controlling the spreading remains the same. In the case of a finite release of fluid (cf. §5), the effect of the capillary retention alters the exponent γ determining the rate of decay of the volume of the current, $V = V_o t^\gamma$. This exponent now depends on both the fraction of fluid retained by capillary effects in the sinking region, and also the fraction of fluid which vaporizes. In figure 11, we present a series of calculations of the dependence of γ on both R and $\mathscr{F}$. It is seen that, as expected, the effect of capillary retention of a part of the descending fluid is to increase the rate of decay of the fluid volume. Indeed, for large values of R and small values of $\mathscr{F}$ the capillary retention may dominate the effect of boiling off of the current. Note that in the present content, this trapped liquid will have a temperature close to the boiling point, leaving a two-phase zone in the wake of the spreading region of liquid.

7. Discussion

The solutions described in §§3–6 all assume that the mass fraction of liquid which vaporizes as the current invades the hot rock is a constant given by (3.1). This condition requires the speed of the liquid front (i) to exceed the rate of heat conduction and (ii) to be smaller than the rate of vapour migration ahead of the front (§1). In each solution we have discussed, the vertical speed of the current has value

$$\frac{\partial h}{\partial t} = H_v D_v^\alpha t^{\alpha-1}\left(\alpha f(\eta) - \beta\eta\frac{df}{d\eta}\right)$$

while the horizontal speed has value $\beta D_v^\beta t^{\beta-1}$. Therefore, except for very rapid injection rates, $\gamma > 2$ (planar) and $\gamma > 3$ (radial), the currents are long and thin. Hence, to determine conditions under which equation (3.1) applies, we compare the vertical ascent speed of the current with the rate of heat transfer $(\kappa/t)^{1/2}$ and the rate of vapour migration $(D_P/t)^{1/2}$. For both planar and axisymmetric currents, two cases arise, depending on the injection rate.
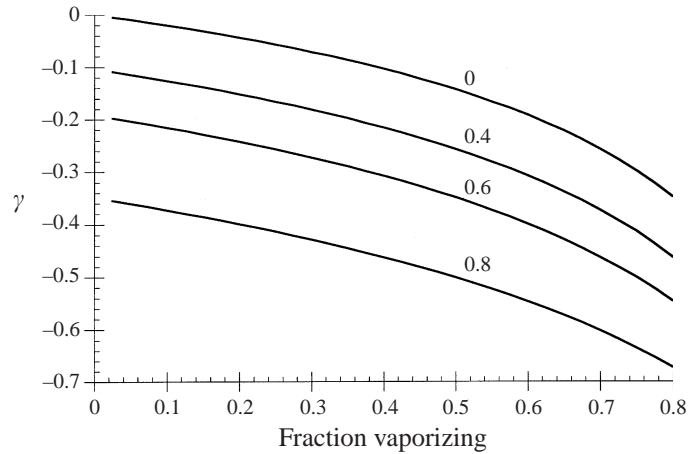
FIGURE 11. Variation of the exponent γ for the volume of a finite release of fluid, $V = V_o(t/t_o)^\gamma$, in the case that a fraction $\mathscr{F}$ of the current vaporizes and that a fraction R (0, 0.4, 0.6, 0.8, as shown on curves) is retained in the pores which are vacated as the current descends.

7.1. *Planar currents*

Comparing the conduction and pressure speeds with the ascent speed of the current, we find that the present model solutions apply for times

$$\left(\frac{D_P}{H_v^2 D_v^{2\alpha}}\right)^{1/(1-2\alpha)} \ll t \ll \left(\frac{\kappa}{H_v^2 D_v^{2\alpha}}\right)^{1/(1-2\alpha)} \tag{7.1}$$

if $\gamma < 5/4$ ($\alpha < 1/2$). As in §3, κ is the thermal diffusion coefficient $\kappa \sim 10^{-6}$ m^2 s^{-1} and $D_P = KP_\infty/\phi\mu$ is the effective vapour diffusion coefficient (cf. Fitzgerald & Woods 1995) with typical values of order $D_P \sim 10^{-1}$–10^{-3} m^2 s^{-1} in a geothermal system of permeability $K = 10^{-12}$ m^2, pressure $P_\infty \sim 10^6$ Pa, void fraction $\phi = 0.1$ and viscosity $\mu = 10^{-4}$ Pa s. Referring to §2, it may be shown that, in the typical case $\mathscr{F} \sim 0.1$–0.5, condition (7.1) reduces to the simpler form

$$D_P^{-1/2} Q_o^{2/3} S^{-1/3} \ll t^{(5-4\gamma)/6} \ll \kappa^{-1/2} Q_o^{2/3} S^{-1/3}, \tag{7.2}$$

where the liquid velocity scale $S \sim 10^{-3}$–10^{-5} m s^{-1} in a geothermal system.

Equation (7.1) identifies that if $\gamma < 5/4$ then the currents propagate relatively slowly and so eventually the effects of heat conduction from the surrounding rock become important. This increases the mass fraction which vaporizes and eventually nearly all of the current vaporizes (cf. Woods & Fitzgerald 1996). We now examine two specific cases to illustrate condition (7.2), which identifies the times (i) before which vapour pressure effects suppress the vaporization; and (ii) after which the effects of thermal diffusion begin to increase the rate of vaporization of the current,

First, consider the case of a constant injection rate so that $\gamma = 1$. Equation (7.2) then takes the form

$$D_P^{-6} Q_o^4 S^{-2} \ll t \ll \kappa^{-6} Q_o^4 S^{-2}. \tag{7.3}$$

Substituting the above values for D_P, κ and S we find that the similarity solutions apply for times 1–$10^4 < t < 10^8$–10^{12} s if $10^{-5} < Q_o < 10^{-4}$ m^2 s^{-1}. This case represents a simplified model of uniform liquid injection from a large horizontal fracture (or horizontal injection well) into an adjoining permeable layer: if the fracture intersects the permeable layer over a length $L \sim 10$–100 m and the current

propagates through the permeable layer away from the fracture, then the total volume injection rate V into the permeable layer, corresponding to LQ_o, would therefore be $10^{-3} < V < 10^{-1}$ m^3 s^{-1}. This lies within the typical range of liquid injection rates into geothermal systems. Therefore, the model can capture a significant part of the spreading of the current. For higher or smaller flow rates, Q_o, the model only applies for very small or very long times.

Next, we consider the evolution of a finite release of fluid Q_oL which is supplied along a length L of a fracture into a permeable layer and which then propagates through the permeable layer away from the fracture (figure 10). As shown in §6, the mass fraction which vaporizes depends on $\mathscr{F}$. If for example $\gamma(\mathscr{F}) = -1/2$, and the planar current has initial volume (at $t = 1$) $10L < Q_o < 10^4L$, then the model (§6.1) applies for times $1\text{--}10^2 < t < 10^2\text{--}10^4$ s. This range of values of Q_o represent currents of initial depth 1–100 m and lateral extent 1–100 m in the permeable layer. At longer times, only a small fraction of order $1/10$ of the initial liquid will remain.

If the injection rate increases with time sufficiently rapidly, $\gamma > 5/4$, then the current propagates so rapidly that the vapour pressure gradually builds up and the mass fraction which vaporizes falls to zero. Now the effects of thermal diffusion are only important at very early times so that the similarity solutions presented herein apply when

$$\left(\frac{\kappa}{H_v^2 D_v^{2\alpha}}\right)^{1/(2\alpha-1)} \ll t \ll \left(\frac{D_P}{H_v^2 D_v^{2\alpha}}\right)^{1/(2\alpha-1)}. \tag{7.4}$$

Note however, that in most practical situations, it is unlikely that the injection rate will increase with time (i.e. $\gamma > 5/4$).

7.2. *Axisymmetric currents*

The range of times for which the approximation $\mathscr{F}$ is constant may again be found by comparing the ascent speed of the current, $\partial h/\partial t$, with the effective thermal and pressure diffusion speeds (cf. (7.1)). In this case we find that if the injection rate $\gamma < 2$, then at long times, thermal diffusion becomes important and vapour pressure effects are negligible (cf. equation (7.1)). It is unlikely that in a practical situation $\gamma > 2$ (cf. (7.4)) and therefore we focus on the case $\gamma < 2$. In this case, the solutions remain valid for times t in the range

$$D_P^{-1}Q_oS^{-1} \ll t^{(2-\gamma)} \ll \kappa^{-1}Q_oS^{-1}. \tag{7.5}$$

We now consider two cases to illustrate the range of validity of the results. First, we consider steady injection $\gamma = 1$ at a rate $10^{-5} - 10^{-2}$ m^3 s^{-1} from a central injection well into a horizontally bounded permeable layer, as is typical of many industrial injection schemes. In this case, the model (§3.2) holds for times t such that $10\text{--}10^4 < t < 10^5\text{--}10^8$ s and may therefore be of considerable practical relevance.

Second we consider the case of a finite release which is then allowed to spread through the reservoir with no further injection. The rate of decay of the current depends on the reservoir superheat. If this is such that, for example $\gamma(\mathscr{F}) = -1/2$ (§5.2), then for a current of initial volume (at $t = 1$) $Q_o = 1\text{--}10^5$ m^3, the model of the spreading and vaporizing current applies for times $1\text{--}10^4 < t < 10^2\text{--}10^6$ s after which time the current mass will have decayed by a factor of about $1/10$. The model (§5.2) therefore provides a useful description of the vaporization and spreading of finite current of initial radial extent 1–100 m and depth 1–100 m.

8. Conclusions

We have presented a new series of similarity solutions to describe the migration of idealized vaporizing gravity currents propagating through a superheated permeable rock. Of particular note, we have shown that for the case of a finite release, the similarity solutions are of the second kind with the mass of the current being proportional to t^γ where γ is a function of $\mathscr{F}$. We have also shown how capillary retention of fluid in the pore spaces can modify these solutions, increasing the decay rate of the current volume in the case of a finite release of fluid. The similarity solutions describe the long time dynamics of the current, to which real currents will tend to converge as they spread from the source.

The present model provides a useful starting point for developing insight and understanding of some aspects of the complex flow dynamics associated with vaporizing liquid currents in geothermal systems. However, it is important to remember that the model is idealized and relaxation of a number of key assumptions merits further investigation. Amongst other real world complicating effects, heterogenities in the structure of the porous rock and regions of the permeable strata dominated by large fractures rather than a uniform porous layer are likely to lead to significant differences in the flow. Also, there is the possibility of viscous instability at the leading edge of the current (cf. Fitzgerald & Woods 1994), the temperature gradient in the environs may not be uniform and as the currents evolve thermal diffusion or the dynamic vapour pressure may become important (§7). We plan to report of some of these issues in future work.

REFERENCES

ARONSON, D. G. & VAZQUEZ, J. L. 1994 Calculation of anomalous exponents in nonlinear diffusion. *Phys Rev. Lett.* **72**, 348–351.

ARONSON, D. G. & VAZQUEZ, J. L. 1995 Anomalous exponents in nonlinear diffusion. *J. Nonlinear Sci.* **5**, 29–56.

BARENBLATT, G. I. 1952 On some unsteady motions of fluids and gases in a porous medium. *Prikl. Mat. Mekh.* **16**(1), 67–78.

BARENBLATT, G. I. 1997 *Self-similarity and Intermediate Asymptotics.* Cambridge University Press.

ENEDY, S. L., SMITH, J. L., YARTER, R. E., JONES, S. M. & CAVOTE, P. E. 1993 Impact of injection on reservoir performance in the NCPA steam field at the Geysers. *Proc. Stanford Geotherm. Workshop,* vol. 18, pp. 125–134.

FITZGERALD, S. D. & WOODS, A. W. 1994 The instability of a vaporization front in a hot porous rock. *Nature* **367**, 450–453.

FITZGERALD, S. D. & WOODS, A. W. 1995 On vapour flow in a hot porous layer. *J. Fluid Mech.* **293**, 1–23.

GRANT, M. A., DONALDSON, I. G. & BIXLEY, P. F. 1982 *Geothermal Reservoir Engineering.* Academic.

HULSHOF, J. & VAZQUEZ, J. L. 1994 Self-similar solutions of the second kind for the modified porous medium equation. *Eur. J. Appl. Maths* **5**, 391–403.

HUPPERT, H. E. & WOODS, A. W. 1995 Gravity driven flows in porous layers. *J. Fluid Mech.* **292**, 55–70.

PATTLE, R. E. 1959 Diffusion from an instantaneous point source with a concentration dependent coefficient. *Q. J. Mech. Appl. Maths* **12**, 407–409.

PHILLIPS, O. M. 1991 *Flow and Reactions in Permeable Rocks.* Cambridge University Press.

PRUESS, K. 1991 Grid orientation and capillary pressure effects in the simulation of water injection into depleted vapour zones. *Geothermics* **20**, 257–277.

Pruess, K., Calore, C., Celati, R. & Wu, Y. S. 1987 An analytical solution for heat transfer at a boiling front moving through a porous medium. *Intl J. Heat Mass Transfer* **30**, 2595–2602.

Woods, A. W. & Fitzgerald, S. D. 1993 The vaporization of a liquid front moving through a hot porous rock. *J. Fluid Mech.* **251**, 563–579.

Woods, A. W. & Fitzgerald, S. D. 1995 Liquid injection into a geothermal reservoir. *Proc. World Geoth Congr., Florence, Italy*, vol. 3, pp. 1293–1298.

Woods, A. W. & Fitzgerald, S. D. 1997 The vaporization of a liquid front moving through a hot porous rock. II. Slow Injection. *J. Fluid Mech.* **343**, 303–316.